

**ABRASIVE-ENTRAINED FORCED PULSED WATERJET TECHNIQUE
BASIC STUDY**

B. Ren, B. Daniels, W. Yan, A. Tieu, and M. Vijay
VLN Advanced Technologies Inc.
Ottawa, Ontario, Canada

ABSTRACT

A new nozzle was developed to generate abrasive-entrained forced pulsed waterjet (AFPJ). Tests were conducted to compare its efficacy with the forced pulsed plain waterjet (FPWJ) and continuous plain waterjet (CWJ) and with abrasives (CAWJ). Garnet and zeolite were used as abrasive material. The area removal rate (A) of paint from aluminum panels (siding) was used as the primary performance indicator. In the range of operating pressures investigated (20.7 to 69-MPa), the results clearly showed that AFPJ performed significantly better than the other three types of jets (FPWJ, CWJ and CAWJ). For example, at the operating pressure of 41-MPa, and water flow rate of 23 litre/min (hydraulic power of 15-kW), the AFPJ removed almost 1.67- m^2/hr of paint compared to 0.46 m^2/hr obtained with the CAWJ. The values of 'A' were virtually zero for FPWJ and CWJ. It should be noted, however, that these results are only preliminary as thorough investigation of this promising technique is still in progress.

1.0 INTRODUCTION

During the past ten years, ultrasonically modulated forced pulsed waterjet (FPWJ) has been successfully employed for several industrial applications (Refs. 1 to 7). Concurrently, abrasive-entrained continuous waterjet (CAWJ) has become equally popular for manufacturing and other applications (Ref. 8). Recently, working on the radiological decontamination projects (Ref. 2), it was realized that combining the beneficial features of both techniques might improve the overall efficiency of decontamination. The most important requirement, especially in responding to emergency situations, is portability of the equipment. Portability depends on compactness, which in turn requires minimum acceptable magnitudes of the operating variables (pressure and hydraulic power). Nozzles to inject abrasives into pulsed waterjet were designed and tested. Performance of the pulsed slurry jet (AFPJ) produced by the nozzles was evaluated based on the removal of paint on aluminum panels (siding), assuming that this method will closely simulate the process (scouring) of decontamination. Brief details of FPWJ, nozzle design and the preliminary results are presented in this paper.

2.0 BACKGROUND

2.1 High-Frequency Forced Pulsed Waterjet (FPWJ)

A detailed description of the FPWJ technique is beyond the scope of this paper. Interested reader, however, can refer to several publications reported in the literature (Refs. 1 to 7). Basically, the technique consists of modulating a continuous stream of water flowing through a simple conical entry nozzle with a centrally located microtip (also called probe). The microtip is attached to a transducer, which is powered by an ultrasonic generator. Figure 1 shows typical views of a regular waterjet (CWJ) and the FPWJ (Ref. 7). When the ultrasonic power is optimum, well-defined fully developed pulsed waterjet is produced. The shape of each pulse is like a mushroom, the size increasing with the standoff distance. The efficacy of the pulsed waterjet stems from the fact that:

- (1) When a pulse impacts on the surface to be treated, the pressure at the point of impact is the waterhammer pressure (p_h), which is equal to: $\rho V_j C_a$ (ρ = density of water; V_j = speed of jet and C_a = speed of sound in water). If the static pump pressure is P , then the amplification of pressure ($M = p_h/P$) is equal to $2(C_a/V_j)$. For example, if the pump were operated at 69-MPa, theoretically, the impact pressure would be of the order of 550-MPa. In practice, however, due to various inefficiencies involved in the process, the impact pressure would be of the order of about 276-MPa, equivalent to an UHP (ultra-high pressure) pump.
- (2) High frequency (20-kHz) of impacts, and
- (3) The diameter of each pulse increases with standoff distance.

The results described in this paper will substantiate these observations.

2.2 CAWJ and AFPJ

Since its development in the early 1980s, the CAWJ technique has advanced most rapidly and has been used for many industrial applications. Once again, details are not given here, as extensive literature exists on the topic (Ref. 8). As explained by Hashish (Ref. 8), several methods have been used for producing CAWJ, the most common one being feeding abrasives through a side port as shown in Fig. 2. However, in the project described here, the main goal was to scour as large an area as possible per pass of the jet over the surface. Therefore, a slightly modified version of the configuration reported by Miller, Kugel and Savanick (Ref. 9) was adopted to produce AFPJ. The method of injection is self-explanatory from Figures 3 and 4. The sizes of the adaptors and the mixing tubes were designed to find out if the jets would effectively scour large areas per pass. The most important consideration in the design was to preserve the characteristics of the water pulses after emerging from the mixing chamber.

3.0 EXPERIMENTAL FACILITY

3.1 Set-up to Produce AFPJ

An overall view of the experimental facility is illustrated in Fig. 5. The set-up basically consisted of the following components:

- High pressure pump
- Abrasive (garnet and zeolite) delivery and metering system; garnet was used only for initial studies (debugging, etc.)
- Pulse waterjet generator (RFM)
- Nozzle assemblies (Fig. 4)
- Air Compressor (used only to purge the lines and to cool the transducer)

High-pressure pump was capable of delivering 53-litre/min of water at the rated pressure of 69-MPa, the maximum hydraulic power (H) being 61-kW.

The abrasive delivery and metering system consisted of a storage hopper, a flow control-metering valve, and a feed hose (old Flow International System). The flow control-metering system was capable of feeding a maximum of 1-kg of zeolite into the mixing chamber, the mesh sizes varying typically from 8 to 200 (4.5-kg for garnet).

The forced pulsed waterjet generator (called, Retrofit Module, RFM) is shown in Fig. 5. The cabinet houses the ultrasonic generator, which when activated, transmits high-frequency electrical pulses to the transducer mounted upstream of the nozzle assembly (black cylinder in the Fig. 4). The other components in the enclosure are control systems that ensure the safety of the operator and also the equipment. For instance, as the transducer requires air-cooling, the purpose of the airflow detector in the enclosure is to make sure that compressed air supply is connected to the RFM. When the RFM is connected to a medium pressure (≤ 138 -MPa) pump of the end-user, it will have the same effect as an UHP on the surface to be treated. Another vital feature of the RFM is its dual mode of operation, that is, if no pulses are required for a particular

application, then there is no need to switch on the ultrasonic generator. RFM in combination with the nozzle assemblies shown in Fig. 4 produced the AFPJ. The ultrasonic power was turned off to obtain the conventional CAWJ (that is, 'pulse-off' mode of operation).

3.2 Properties of Abrasive Material

Garnet and zeolite were used as abrasive material. As garnet was used only for debugging the system, description of its properties is not given here (see the citations in Ref. 8).

Zeolite (Clinoptilolite) is a naturally occurring mineral made of a special crystalline structure that is porous but remains rigid in the presence of water (Ref. 10). Zeolites can be adapted for a variety of uses (aquaculture, agriculture, horticulture, household and industrial products, radioactive waste, water and wastewater treatments). Compositionally, zeolites are similar to clay minerals. More specifically, both are aluminosilicates. They differ, however, in their crystalline structure. Many types of clay have a layered crystalline structure (similar to a deck of cards) and are subject to shrinking and swelling as water is absorbed and removed between the layers. In contrast, zeolites have a rigid, 3-dimensional crystalline structure (similar to a honeycomb) consisting of a network of interconnected tunnels and cages (Fig. 6). Water moves freely in and out of these pores, but the zeolite framework remains rigid. Another special aspect of this structure is that the pore and channel sizes are nearly uniform, allowing the crystal to act as a molecular sieve. The porous zeolite is host to water molecules and ions of potassium and calcium, as well as a variety of other positively charged ions, but only those of appropriate molecular size to fit into the pores are admitted creating the "sieving" property.

One important property of zeolite is the ability to exchange cations. This is the trading of one charged ion for another on the crystal. One measure of this property is the *cation exchange capacity* (CEC). Zeolites have high CEC's, arising during the formation of the zeolite from the substitution of an aluminum ion for a silicon ion in a portion of the silicate framework. High CEC plays a vital role in adsorption of radioactive particles. There are nearly 50 different types of zeolites (clinoptilolite, chabazite, phillipsite, mordenite, etc.) with varying physical and chemical properties. Crystal structure and chemical composition account for the primary differences. Particle density, cation selectivity, molecular pore size, and strength are only some of the properties that can differ depending on the zeolite in question. Finally, one difference between zeolites worth giving special mention is the composition of exchangeable cations residing in the zeolite. Exchange sites on natural zeolites are primarily occupied by 3 major cations: potassium (K), calcium (Ca), and sodium (Na). Other elements such as magnesium (Mg) may also be present. Exchange sites on a particular zeolite may contain nearly all K, nearly all Na, some Ca or Mg, or a combination of these. It is important to take these differences into account when assessing which zeolite to use for a particular application (in the present case, adsorption of radioactivity).

Two different sizes of zeolites, -80 powder and coarse (medium-size; 20 to 40-mesh), were used in the project. The supplier did not furnish specific details of their properties. However, compared to garnet (mesh = 80, density = $3.4 - 4.3 \times 10^3$ -kg/m³ and hardness ≈ 7.5 -Moh), zeolite is quite soft (3.5 - 4-Moh) and light ($0.74 - 0.82 \times 10^3$ -kg/m³). Furthermore, the shape of the particles was quite smooth, not irregular like garnet.

4.0 EXPERIMENTAL PROCEDURE AND PRESENTATION OF RESULTS

4.1 General Remarks

Garnet was used to debug the nozzle configuration. For this purpose samples of HDPE (high density polyethylene) were used to measure the mass loss rate (ΔM). ΔM was obtained as a function of the pressure (P), orifice diameter (d, that is, water flow rate, M_w), abrasive flow rate (M_a), standoff distance (S), and the traverse speed (V).

For evaluating the performance of AFPJ, samples of commercially available painted aluminum siding were used (actually to simulate the scouring of radioactive particles from a surface). The thickness of the polyester paint, which was baked on at 238°C, was about 0.02-mm.

4.2 Test Procedure

The experimental procedure was quite simple. Once the required orifice and the nozzle assembly were assembled, the magnitudes of the operating pressure and the abrasive flow were set to the required values. The nozzle assembly was then traversed over the samples (set at several standoff distances) at varying traverse speeds. In the case of HDPE, the mass loss was measured. For painted samples, the widths of paint removed and quality of the substrate were recorded. Only those data in which the substrate was not damaged were considered useful in plotting the area removal rates (A) against the operating parameters. In order to observe if pulsing is better than continuous waterjet, for each value of abrasive flow rate ($M_a = 0$ implies plain waterjet), tests were conducted with pulse on (CWJ, CAWJ) and pulse off (FPWJ, AFPJ). All tests were conducted on the X-Y gantry.

4.3 Presentation of Results

Following the procedure stated above, plots of ' ΔM ' are presented first followed by the plots of 'A'. A few photos (qualitative results; Figs. 7, 8 and 9) of the samples exposed to jets are illustrated to elucidate the effect of abrasives in the jets. ΔM results are shown in Figs. 10 and 11. Area removal results appear in Figs. 12 to 15. As pointed out elsewhere, the results are only preliminary. For example, the results presented here were obtained with the assembly of pulsing nozzle and the mixing chamber only (except the couple of results shown in Fig. 7B).

5.0 DISCUSSION

5.1 Qualitative Observations (Figs. 7, 8 and 9)

Figure 7(A) shows typical appearance of HDPE samples eroded by waterjets emerging from the mixing chamber only (see Fig. 4). The enhanced performance of 80-mesh garnet-entrained AFPJ can be readily recognized. The magnitude of ΔM was 41.3-g/min compared to 14.3-g/min obtained with the CAWJ {indicated by P 'off', A (abrasive) 'on'}, an increment by a factor of three. However, when compared to the FPWJ (P 'on', A 'off'), the performance increased only

by 12.5 percent. This is because the slurry is quite dilute ($C < 3\%$), and there would be a significant improvement if the concentration were increased (Ref. 8).

Figure 7(B) shows the effect of adding the adaptor (#1) to the mixing chamber on ΔM for the same operating conditions. As expected, the magnitude of ΔM decreased due to increased friction in the adaptor. On the other hand, the area eroded by the jet has increased significantly (compare Test #106 with #73). This is precisely the premise for designing the nozzle configurations, namely to scour as large an area as possible per pass of the jet over the surface. Further work is in progress to assess the effect of all the components depicted in Fig. 4.

Figures 8 and 9 clearly show the effect of zeolite (-80-powder)-entrained AFPJ on the surface finish (with the mixing chamber only), at operating conditions as indicated. At the same standoff distance and traverse speed, when the pressure was increased from 27.6 to 41.4-MPa, AFPJ almost cut the substrate, even though the concentration was less than 3.5% (Fig. 8). Although the concentration is low, it is quite likely that zeolite-particles being light fill the entire cross section of the pulsed jet. Thus, as in the case of mass loss, this observation confirms that the AFPJ is quite effective for removing the paints. The damage to the substrate can be eliminated either by increasing the traverse speed (in automated applications), or keeping the pressures below 30-MPa (in hand-held operations).

In Fig. 9, the effects of standoff distance, the traverse speed and the size of the mesh (powder for Tests #5A to 9C; Coarse for 27C and 28C) on surface finish are indicated ($V = 1.27\text{-m/min}$ for Tests #5A, B and C; $V = 3.6\text{-m/min}$ for Tests #9A, B and C). The highlights are:

1. For a given traverse speed, when the standoff distance is increased from 12.7 to 63.5-mm the width of the swath of paint removed increases from 8 to 12-mm, although not as much as one would have expected (the size of the pulses increase with standoff, see Fig. 1).
2. For a given standoff distance (e.g., 12.7-mm; Tests #5A to 9A), the width of the swath decreased from 8 to about 6-mm with the increase in traverse speed (from 1.27 to 3.6-m/min).
3. Comparison of the swaths obtained with the powder (Tests #5A to 9C) and those with the coarse zeolite (Tests #27C & 28C), seems to indicate that the former does not erode the substrate even at the low traverse speed of 1.27-m/min. The latter appeared to be more aggressive and damaged the substrate, even though the pressure was lower (34.5-MPa) and the traverse speed much higher (1.9-m/min; pits are clearly visible). Therefore, from the standpoint of removing the paint without damaging the base metal, the powder certainly seems to be better (if coarse material is employed, traverse speeds must be substantially greater than 1.9-m/min; see the discussion related to Fig. 15).

5.2 Quantitative Observations: ΔM Results (Figs. 10 and 11)

Figure 10:

In this plot data are plotted as a function of abrasive concentration at a constant flow rate of water (29.5-litre/min) and traverse speed (1.27-m/min) at two different values of pressure (34.5 and 69-MPa). In CAWJ technique, the function of the waterjet, after intermingling with the

particles in the mixing chamber, is to accelerate the speed of the particles (Ref. 8). Ideally, the maximum speed of the particles would be the same as that of the jet. However, due to frictional effects and other factors in the mixing chamber, the speed is always less than that of the jet. Nonetheless, the speeds at which the particles impact the target augment the erosive power of the jet. As the speed of the jet is a function of the pressure ($V_j = kP^{1/2}$; $k = \text{constant}$), particles would be much more aggressive at higher pressures. This is quite evident from the results in this plot. Important observations from this plot are:

- The data indicate that AFPJ certainly removes more material than the CAWJ. However, it appears that there is a threshold pressure below which the improvement is not significantly better for cutting. This is evident from the data at 34.5-MPa.
- At 69-MPa, the AFPJ removed ≈ 40 -g/min (at $C \approx 8\%$) compared to 30-g/min by the FPWJ ($C = 0\%$). The trend of the data indicates the performance would increase significantly if the concentration were increased beyond 8 percent.
- At 69-MPa, the AFPJ removed 40-g/min compared to 15-g/min removed by the CAWJ, a significant improvement by a factor of 2.7. Considering that the concentration is less than 10%, this is highly encouraging (for low concentrations abrasive feeding systems would be quite simple).
- At 34.5-MPa, the results are somewhat anomalous, although the performance of AFPJ is still slightly better than that of the CAWJ. The performance appears to decrease when the concentration increases from 0 to about 4 percent. This is probably due to frictional effect in the process of mixing in the chamber.

Figure 11

In this plot, ΔM data are plotted against concentration to observe the effect of water flow rate (37.8 and 55-litre/min) on performance at a constant pressure (46.9-MPa). First, it should be noted that the value of C could not be raised beyond 3.5% and 6% when the flow rates were respectively 55 and 37.8-litre/min. The reason for this is, for the nozzle configuration used in the present investigation, pressure in the mixing chamber builds up as the water flow increases (the flow will also be highly turbulent). Consequently, suction of abrasives would decrease. Other observations from this plot are:

- The data once again confirm the superior performance of AFPJ compared to the corresponding CAWJ.
- Increasing the flow rate from 37.8 to 55-litre/min (by 46%) increases the magnitude of ΔM from 26 to 28 g/min (taking the peak values), that is, only by 8 percent. This would indicate increasing the water flow rate eventually deteriorates the performance.

- Another way of examining the relative performance is by comparing the specific energies (energy used to remove a gram of material = $E = H/\Delta M$). Using the data in this and Fig. 10, the results are:

P (MPa)	Q (Litre/min)	H (kW)	ΔM (g/min)	E (kW-min/g)
34.5	29.5	17.2	5.0	3.4
46.9	37.8	29.8	26.0	1.1
46.9	55.0	43.2	28.0	1.5
69.0	29.5	34.3	38.0	0.9

Clearly, the minimum value of E occurs for 69-MPa and 29.5-litre/min. Therefore, at least from the standpoint of cutting materials, for a given hydraulic power, it is better to use higher pressures than water flow rates.

5.3 Quantitative Observations: Paint Removal Results (12 to 15)

Figure 12

In this Figure values of 'A' are plotted against C for a constant pressure of 34.5-MPa and other parameters as indicated. The highlights from this plot are:

- For both sizes of zeolite (medium and powder), the performance of AFPJ is significantly superior to that of the CAWJ. For instance, with the powder zeolite, the peak value achieved with the AFPJ is of the order of 1.1 m²/hr compared to 0.46 m²/hr for the CAWJ (for the medium size, the improvement is ≈ 3 times).
- The magnitudes of 'A' are basically equal for both meshes up to $C \approx 3.5\%$. However, for the powder, the trend of the data indicates that 'A' could increase significantly with the increase in concentration. Since the medium size particles tend to erode the metal (see Fig. 9), powder would be more beneficial.
- For CWJ or FPWJ ($C = 0$), the value of 'A' is almost zero.

Figure 13

This plot shows the effects of: (1) pulse on/off and (2) pressure at constant water flow rate of 25-litre/min. First, it is interesting to note that the performance of AFPJ at 21-MPa is equivalent to that of the CAWJ at 47-MPa, undoubtedly confirming the superior performance of AFPJ. With respect to the effect of pressure, although the area removal rate increases with pressure, it is not as remarkable as found in the case of cutting plastic samples (see Fig. 10). At 21-MPa and 25-litre/min, the hydraulic power is only 8.6-kW, and therefore, from the standpoint of simplicity of the complete system (compact and portable), removal of paints at lower pressures seems more appealing and economical (especially for handheld tasks).

Figure 14

In this plot, the effects of both flow and pressure on 'A' are indicated. Once again, the plot clearly confirms the superior performance of AFPJ. However, if the data at 41-MPa (23-

litre/min) are compared with those obtained at 47-MPa (25-litre/min), it is clear that the performance has not increased significantly (at concentrations > 4%, the performance is almost the same). This observation, just as in the case of ΔM , suggests that there are optimum sets of operating parameters at which the specific energy $\{E_a = \text{power}/A, \text{ kW-hr/m}^2\}$ will be minimum. This is indicated in the following table.

P (MPa)	Q (Litre/min)	H (kW)	A (m ² /hr)	E _a (kW-hr/m ²)
21.0	25.0	8.6	0.63	13.6
34.5	21.2	12.2	1.09	11.2
34.5	29.5	17.0	1.04	16.3
41.0	23.0	16.0	1.39	11.5
47.0	25.0	19.5	1.10	17.7

Thus, although 41-MPa (16-kW) yields maximum value of 'A', from the standpoint of specific energy, operation at 34.5-MPa (12.2-kW) would be equally effective. The trend of the data at these operating conditions appears to indicate the magnitude of 'A' would increase with the concentration (> 5%).

Figure 15

In this plot, the effect of coarse zeolite on performance is indicated explicitly. In Fig. 12, at 34.5-MPa, there is no significant difference between the powder and the medium size zeolite (up to $C \approx 4\%$). However, at 41-MPa & 23-litre/min, the medium size seems to perform significantly better than the powder (see Fig. 14 for powder). For instance, at $C \approx 4\%$, the magnitude of 'A' is about twice that of the powder. Since $V = 3.3\text{-m/min}$, the substrate was not affected (see Fig. 8 for damage at $V = 2\text{-m/min}$). Therefore, it is quite likely at higher pressures the coarse zeolite is probably better than the powder for removing the paint. Once again, the superior performance of AFPJ compared to CAWJ is quite evident.

6.0 CONCLUSIONS

The main goal of the project was to determine if pulsed zeolite-entrained slurry jet would be suitable for radiological decontamination. In this preliminary investigation, paint removal tests were conducted assuming that this method will closely simulate scouring of radioactive particles from surfaces. Four modes of operation were investigated: CWJ, CAWJ, FPWJ and AFPJ. The main conclusions from this limited investigation are:

- The nozzle configuration, although designed somewhat on an *ad-hoc* basis, did produce an acceptable zeolite-entrained pulsed slurry jet (AFPJ).
- In cutting tests, the efficacy of the garnet-laden AFPJ is almost three times that of a conventional CAWJ.
- Surprisingly, the concentration of abrasives is quite low (< 6%). While this is a good sign (system requirements will be minimal), the trends of data do indicate that the efficacy can be improved significantly by increasing the concentration (>10%).

- With respect to paint removal, erosion (wear and tear) of the surface can be avoided by using appropriate set of operating parameters (indicated by the surface finish of aluminum).
- The optimum magnitudes of pressure and flow appear to be in the range of 34.5 – 41-MPa and 21 – 23 litre/min (specific energy in this range is $\approx 11\text{-kW-hr/m}^2$). Systems at these low pressures will be compact, which are desirable for many applications.
- The mesh size appeared to have some effect on the performance, coarse zeolite being significantly better than the powder at higher pressures. However, appropriate traverse speed must be selected to avoid erosion of the substrate.
- The performance remained fairly constant over a range of standoff distances from 12.7 to 63.5-mm. In handheld operations this will be highly beneficial.

7.0 REFERENCES

1. Yan, W., A. Tieu, B. Ren and M. Vijay, "High-Frequency Forced Pulsed Waterjet Technology for the Removal Coatings," JPCL (Journal of Protective Coatings & Linings), V.20, No.1, January 2003, pp. 83-99.
2. Vijay, M.M., "Doing More With Less: Pulsed Jet Technique, Part One," Cleaner Times, February 2005, pp. 28-31.
3. Vijay, M.M., "Doing More With Less: Pulsed Jet Technique, Part Two," Cleaner Times, March 2005, pp. 40-43.
4. Vijay, M.M., "Ultrasonically Generated Cavitating or Interrupted Jet," US Patent No. 5,154,347, October 13, 1992; Canadian Patent No. 2035702, October 01, 1996.
5. Vijay, M.M., W. Yan, A. Tieu and B. Ren, "Ultrasonic Waterjet Apparatus," International Publication Number: WO 2005/042177, May 12, 2005.
6. Vijay, M.M., "Pulsed Jets: Fundamentals and Applications," Proc. 5th Pacific Rim International Conference on Water Jet, Technology (New Delhi, India), Water Jet Technology Society of Japan, Tokyo, Japan, 1998, pp. 610-627.
7. Vijay, M.M., Lai, M.K.Y., and Jiang, M., "Computational Fluid Dynamic Analysis and Visualization of High-Frequency Pulsed Waterjet," Proc. 8th American Waterjet Conference (Houston, USA), Waterjet Technology Association, St. Louis, USA., 1995, pp. 557-572.
8. Hashish, M., "Abrasive-Waterjet (AWJ) Studies," Proc. 16th International Conference on Water Jetting (Aix-en-Provence, France), BHR Group Limited, Cranfield, Bedfordshire, England, 2002, pp. 13-47.
9. Miller, A.L., R.W. Kugel and G.A. Savanick, "The Dynamics of Multi-Phase Flow in Collimated Jets," Paper No.18, Proc. 5th American Waterjet Conference (Ottawa, Canada), Waterjet Technology Association, St. Louis, USA., 1989, pp. 179-189.

10. Dyer, A., "An Introduction to Zeolite Molecular Sieves," John Wiley, UK, 1988.

8.0 ACKNOWLEDGMENTS

The authors gratefully acknowledge the partial funding received from the CBRN/CRTI Directorate, and the CRA (SR&ED credit), Government of Canada, for this project. Particular thanks are due to Dr. M. Fingas (Environment Canada), Project Manager for the project, Dr. T. Cousins (DRDC-Ottawa), Leader of Radiation Technologies, Dr. D. Haslip (DRDC-Ottawa) and Mr. T. Jones (DRDC-Ottawa) for their continuing encouragement and technical input. It is a pleasure to acknowledge Mr. W. Bloom and Mr. A. Marsh, VLN Tech., for their administrative support.

(CBRN/CRTI: Chemical, Biological, Radiological and Nuclear/Canadian Research Technology Initiative; CRA: Canada Revenue Agency; SR&ED: Scientific Research & Engineering Development, DRDC: Defence R&D Canada, Department of National Defence).

9.0 NOMENCLATURE

A:	Area removal rate of paint, m ² /hr
AFPJ:	Abrasive-entrained forced pulsed waterjet
C:	Concentration of abrasives = M_a/M_w , (%)
CAWJ:	Abrasive-entrained continuous waterjet
CWJ:	Continuous plain waterjet
d:	Waterjet orifice diameter, mm
E:	Specific energy, kW-min/g or kW-hr/m ²
FPWJ:	Forced pulsed plain waterjet
H:	Hydraulic power, kW
M_a	Mass flow rate of abrasives, kg/min
M_w	Mass flow rate of water, kg/min
P:	Pressure of pump, MPa
Q:	Flow rate of water, litre/min
S:	Standoff distance, mm
V:	Traverse speed of jet, m/min
W:	Width of swath of paint removed, mm
ΔM :	Rate of mass loss exposed to the jet, kg/min

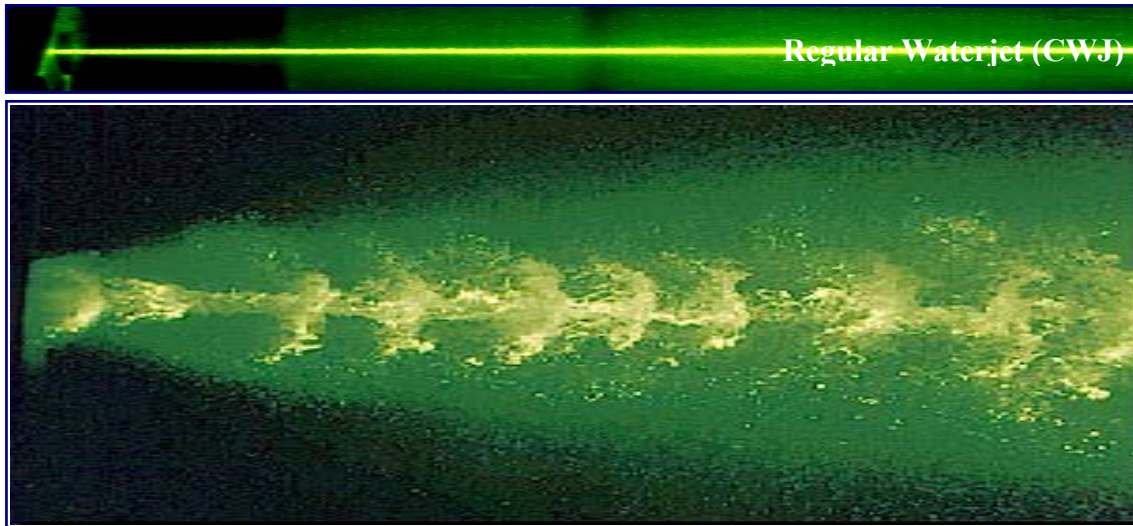


Fig. 1. Typical views of CWJ and FPWJ taken with a short duration (4 to 6-ns) Nd – Yag laser.

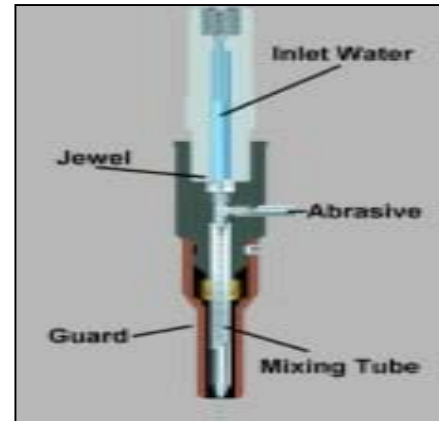


Fig. 2. Conventional CAWJ system.

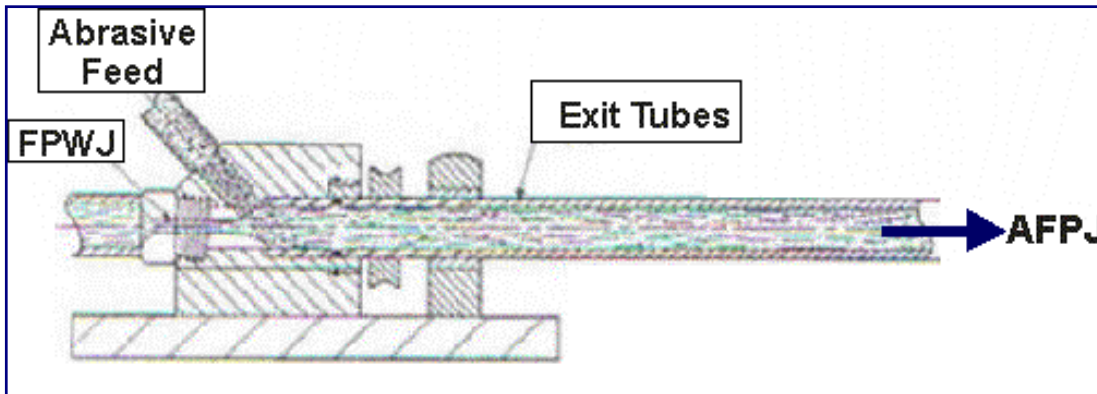


Fig. 3. Method used for injecting abrasives into the stream pulses to generate AFPJ (Ref. 9).



Fig. 4. A general view of the components fabricated for producing AFPJ.

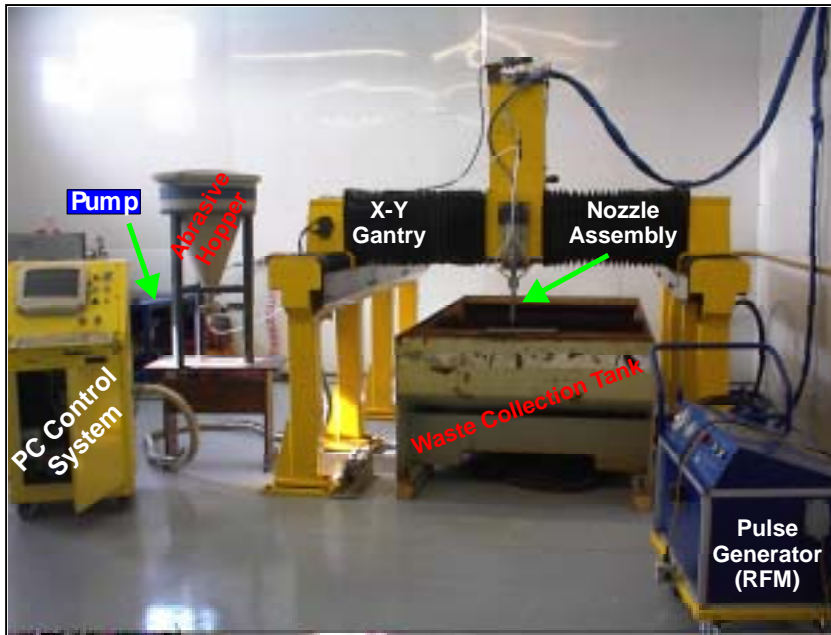


Fig. 5. A general view of the experimental set-up

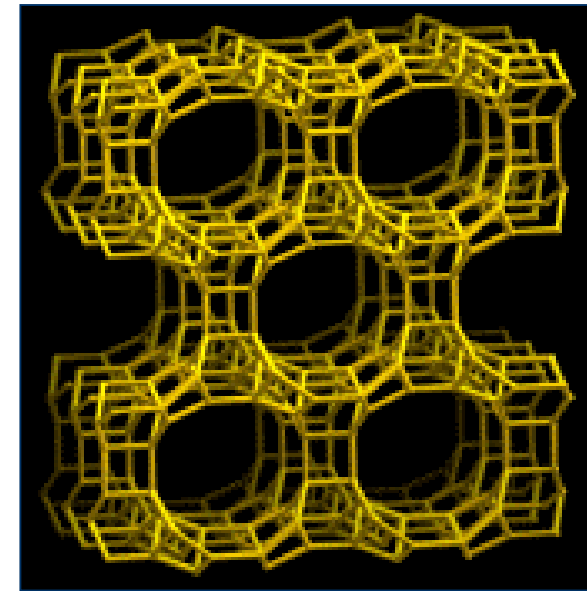


Fig. 6. Clinoptilolite framework model – view along cleavage plane of crystal plates, showing pores and atomic clusters (generally Potassium, Calcium and Sodium, which are cations).

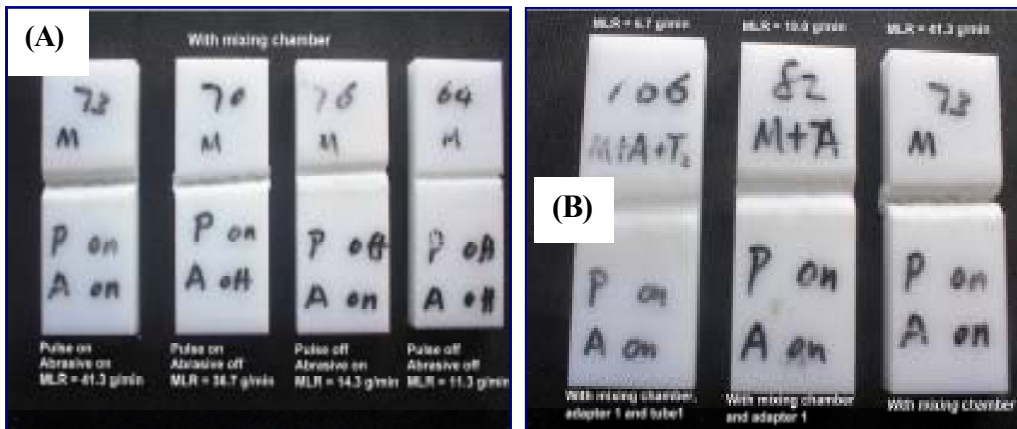


Fig. 7. A close-up view of the HDPE samples exposed to the AFPJ (garnet). (A) Effect of four-modes of operation. (B) Effect of nozzle configuration (see Figs. 3 & 4).

P = 69-MPa, Q = 45.8-litre/min and C = 2.0%.

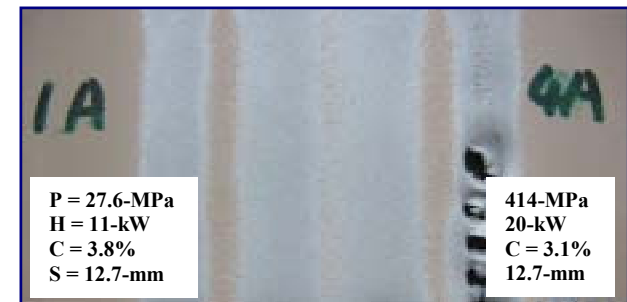


Fig. 8. Tests conducted at 2-m/min with zeolite (-80-powder). At 41-MPa, the sample was cut at several spots by AFPJ.

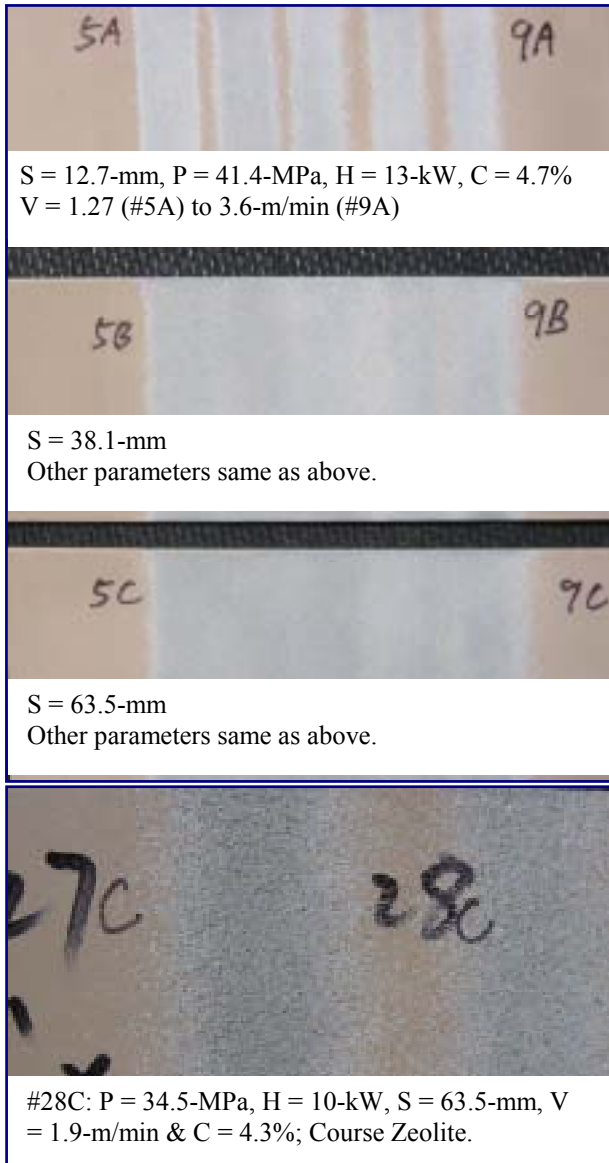


Fig. 9. Surface finish at various operating conditions as indicated with powder (#5A to #9C) and coarse zeolite.

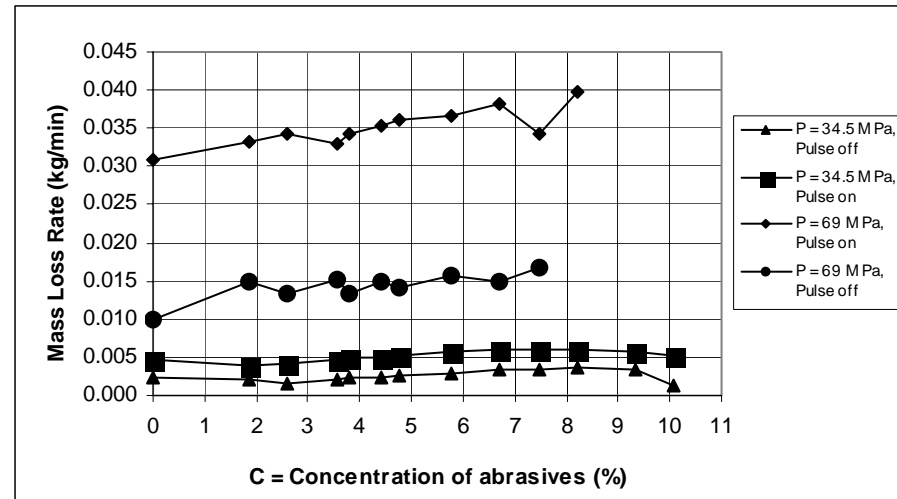


Fig. 10. Plot of MLR against C showing the effect of pressure at constant water flow rate $Q = 29.5$ litre/min.

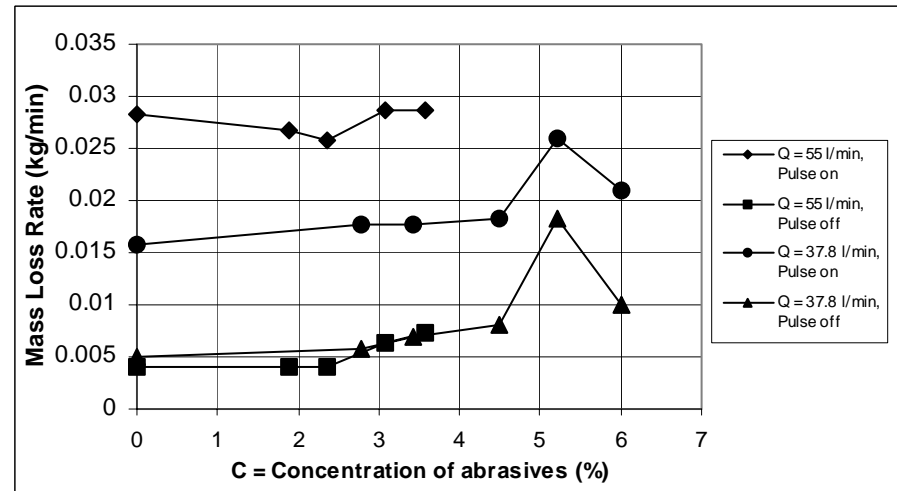


Fig. 11. Plot of MLR against C showing the effect of water flow rate at constant pressure of 46.9 MPa

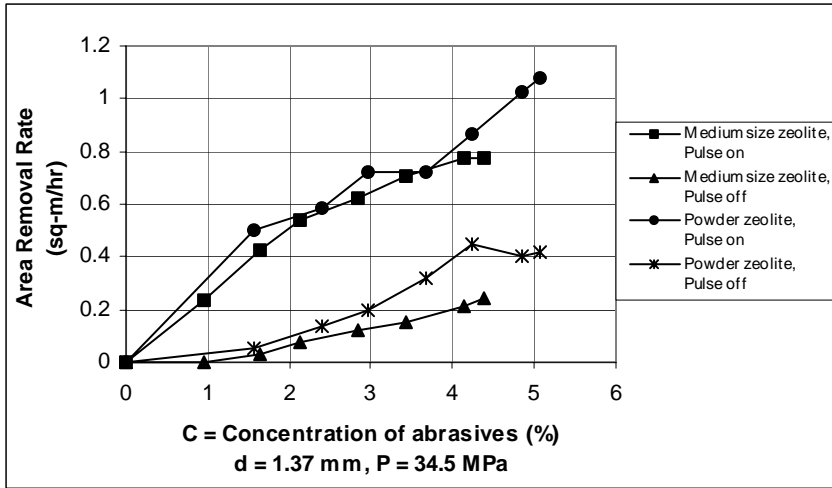


Fig. 12. Plot of A against C showing the effect of: (1) mesh size and (2) pulse on (AFPJ) /off (CAWJ).

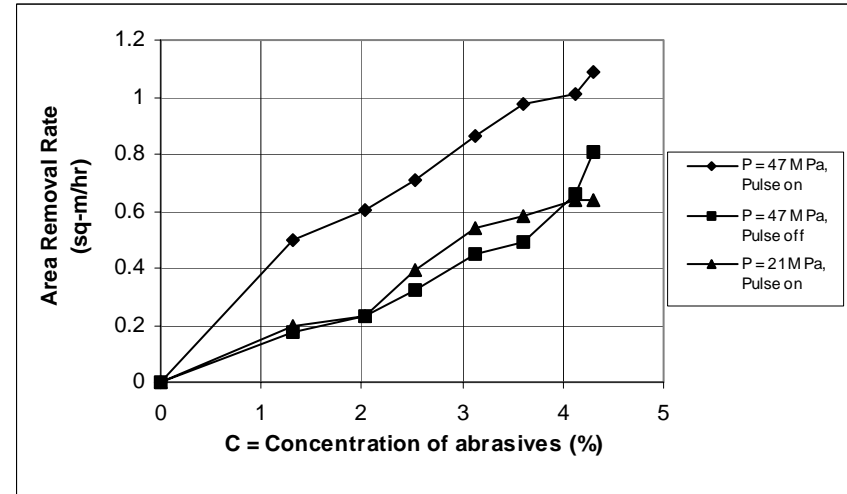


Fig.13. Plot of A against C showing the effect of pressure at a constant water flow rate of 25 l/min.

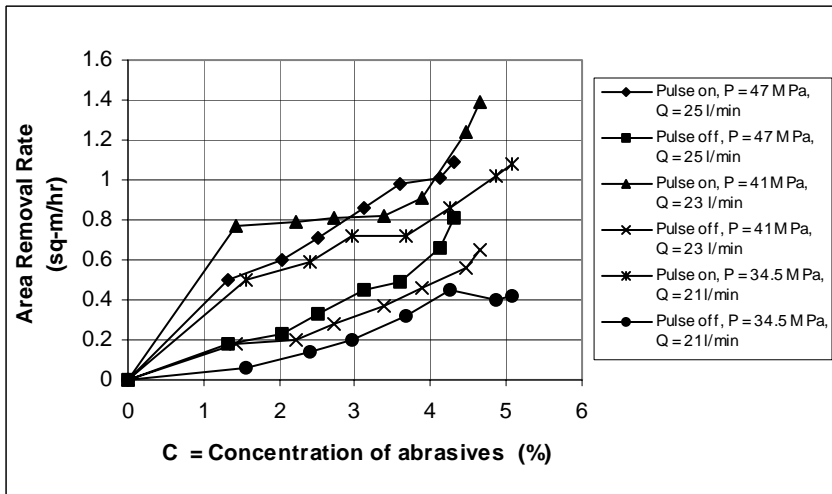


Fig. 14. Plot of A against C showing the effect of pressure at a constant nozzle diameter of 1.37 mm: Powder Zeolite.

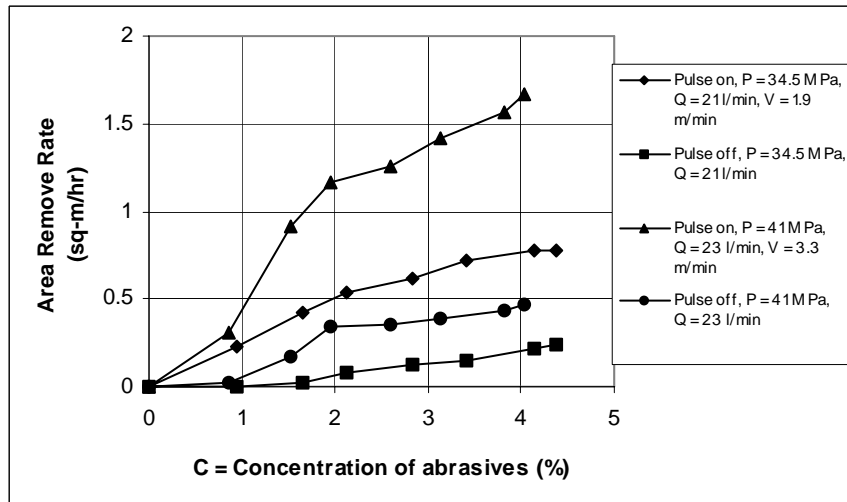


Fig. 15. Plot of A against C showing the effect of pressure at a constant nozzle diameter of 1.37 mm: Coarse Zeolite.